

Temperature Dependency of Ytterbium-Doped Fiber Laser (YDFL) Based on Fabry-Perot Design Operating at 915 nm and 970 nm High Power Pumping Configuration

Fady I. El-Nahal¹, Abdel Hakeim M. Husein²

¹Electrical Engineering Department, Islamic University of Gaza, Gaza, Palestine

fnahal@iugaza.edu.ps

²Physics Department, Al Aqsa University, Gaza, Palestine.

Abstract— The variation of the output power of Ytterbium-doped fiber lasers (YDFLs) with temperature has been evaluated. Temperature-dependent rate equations of ytterbium fiber laser based on Fabry-Perot design have been discussed. The results demonstrate that the output power decrease with the increase of temperature. The effect of the temperature on the output performance increases by increasing the pump power. The effect of temperature can be ignored only for lower pump power. The theoretical result is in agreement with the published experimental results.

Index Terms— Ytterbium-doped fiber laser, Temperature-dependent rate equation.

1. INTRODUCTION

Since the first report in 1962 of laser achievement in ytterbium ion (Yb^{3+}) doped silicate glass [1]. Ytterbium (Yb)-doped fiber lasers (YDFLs) have attracted great interest because they offer the advantages of compact size and structure, high gain, guided mode propagation, highly stable processes, their outstanding thermo-optical properties and high doping levels are possible [1-6]. Moreover, It does not have some of the drawbacks associated with other rare-doped fiber such as excited state absorption phenomenon that can reduce the pump efficiency and concentration quenching by interionic energy transfer. Thus, it offers high output power (or gain) with a smaller fiber length. YDFA's have a simple energy level structure and provide amplification over a broad wavelength range from 915 to 1200 nm. Furthermore, YDFA's can offer high output power and excellent power conversion efficiency [1,7,8].

Lately, interest has been shown in Yb^{3+} as a laser ion, in the form of Yb^{3+} -doped silica and fluoride fiber lasers [9]. YDFLs have been widely used in advanced manufacturing, high energy physics and military defense [10]. There are several theoretical analyses of the YDFL based on rate equations and power differential transmission with fixed or variant parameters of the fiber laser, the results of which are important for optimization of fiber lasers. The numerical analysis of thermal distribution and its effects on the high power YDFLs have been studied, as thermal damage, refractive index variation of the gain fiber, and output wavelength [11]. Several papers studied the temperature effects on the output performance of YDFLs. It is reported that the central wavelength of output laser shifts to longer wavelength and the output power decrease with increase of temperature [12, 13]. Brilliant et. al. showed their experimental results of tempera-

ture tuning in a dual-clad ytterbium fiber laser, they varied the temperature of the fiber from 0 to 100°C and found important changes in operating wavelength, power and threshold [14].

Today, the wavelength shift can be controlled with the using of fiber grating. Thus the temperature-dependence study about fixed wavelength is required. The effect of temperature on the optical properties of YDF lasing at different wavelengths has been analyzed [15]. Nevertheless, to our knowledge, there is no articles that discuss the effect of temperature on the best possible conditions of YDFLs theoretically so far. In this article, the temperature-dependency model based on ions' rearrangement emerging from temperature variation for YDFLs with two-end Fabry-Perot mirrors has been presented. In this model, the output performance can be studied (slope efficiency and the output power) depending on the temperature. In addition, the heat distribution along the laser cavity, and the numerical results of slope efficiency are combined. The optimal fiber length is obtained by taking into account the variation of temperature.

2- THEORETICAL MODEL

The energy level system for Yb having possible transitions is shown in Figure 1 [16]. The effect of the temperature on the ion distribution between upper and lower energy level within a manifold is considered. However, the redistribution of ions between the excited manifold $^2\text{F}_{5/2}$ and the ground manifold $^2\text{F}_{7/2}$ is ignored. This can be justified because of the large energy gap between these two manifolds, on the basis of Boltzmann distribution and the energy level diagram. The standard rate equations for two-level systems are used to describe the gain and propagation characteristics of the fiber

laser because the ASE power is negligible for a high power amplifier with sufficient input signal (about 1 mW). After the overlap factors are introduced and the fiber loss ignored, the simplified two-level rate equations and propagation equations are given as follow [17]

$$\frac{dN_2}{dt} = (W_{12p}f_{lp} - W_{12s}f_{up})N_1 - (W_{21p}f_{up} + W_{21s}f_{us} + A_{21}f_{us})N_2 \quad (1)$$

where W_{12} and W_{21} are the stimulated absorption and stimulated emission transition probability, respectively. They can be given as:

$$W_{12p} = \frac{\Gamma_p \sigma_{ap} P_p}{Ah\nu_p}; \quad W_{12s} = \frac{\Gamma_s \sigma_{as} P_s}{Ah\nu_s} \quad (2)$$

$$W_{21p} = \frac{\Gamma_p \sigma_{ep} P_p}{Ah\nu_p}; \quad W_{21s} = \frac{\Gamma_s \sigma_{es} P_s}{Ah\nu_s}; \quad A_{21} = \frac{1}{\tau} \quad (3)$$

where $P_s(z,t)$, $P_p(z,t)$ are the signal and pump power respectively. σ_{as} and σ_{es} are the signal absorption and emission cross sections. ν_s and ν_p are the frequencies of signal and pump light, respectively. h is Planck's constant. A is the doped area of the fiber. A_{21} is the spontaneous radiation transition probability and τ is the upper state lifetime. Γ_s and Γ_p are the overlapping factor of laser power and the pump power, respectively. $\Gamma_s(\lambda_s)$ is given by $1 - e^{-V}$, where V can be obtained by $2\pi a^2 NA / \lambda_s$, where NA is the numerical aperture. Γ_p can be approximately got by $(a/b)^2$. a and b refer to the radius of the fiber core and the radius of the inner cladding of the YDF [18].

Level	Energy [cm ⁻¹]
a	0
b	492
c	970
d	1365
e	10239
f	10909
g	11689

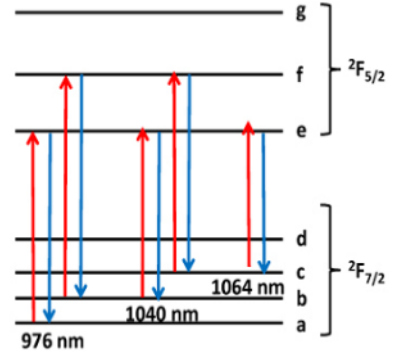


Figure1 Energy level diagram of Yb in silica with 976 nm, 1040 nm, and 1064 nm transitions labeled.

Source: [24]

The Yb- dopant concentration is N_t , and given by[19];

$$N_1 + N_2 = N_t \quad (4)$$

where N_1 and N_2 are the ground and upper-level populations.

The energy level diagram for Yb in silica may vary with each individual fiber. Because of the splitting of the levels depends on the glass composition, concentration of dopants and co-dopants, and the degree of structure disorder of the glass network. The absorption and emission cross-sections for Yb in silica are related to the temperature and the energy of the levels[20]. The saturation of ytterbium absorbing transition occurs when population of two stark levels involving in the transition are matched. The photon energy is the energy difference between the highest Stark level of the ground state $^2F_{7/2}$ (4) and the lowest Stark level of the excited state $^2F_{5/2}$ (1) of the Yb^{3+} ion in phosphate glass. Therefore, we assume in the model that just these two sublevels and calculate the Boltzmann occupation factors f_{li} and f_{ui} of lower and upper manifolds for lower and upper levels from measured stark splitting E_i and E_j and they can be expressed as [21-23]

$$f_{li} = \frac{e^{-E_i/K_B T}}{\sum_{i=1}^4 e^{-E_j/K_B T}} \quad \text{For Yb ground state} \quad (5)$$

$$f_{ui} = \frac{e^{-E_i/K_B T}}{\sum_{j=1}^3 e^{-E_j/K_B T}} \quad \text{For Yb excited state} \quad (6)$$

K_B is Boltzmann's constant and equals 1.38×10^{-23} J/K. At steady state, $dN_2 / dt = 0$, then

$$N_2 = \frac{(W_{12p}f_{lp} - W_{12s}f_{up})}{(W_{21p}f_{up} + W_{21s}f_{us} + A_{21}f_{us})} N_1 \quad (7)$$

$$\frac{N_2}{N} = \frac{(W_{12p}f_{lp} + W_{12s}f_{ls})}{(W_{21p}f_{lp}N_1 + W_{21s}f_{ls}N_1 + W_{21p}f_{up} + W_{21s}f_{us} + A_2f_{us})} \quad (8)$$

where the subscripts s and p represent laser and pump, respectively.

At the same time, by considering the scattering losses both for pump and laser, and then the power time independency differential transmission equations considering temperature by ignoring the amplified spontaneous emission (ASE) can be expressed as follows:

$$\frac{dP_p(z)}{dz} = \Gamma_p N_2 \left[(\sigma_{up}f_{lp} + \sigma_{ep}f_{up}) - \sigma_{up}f_{lp}N \right] P_p(z) - \alpha_p P_p(z) \quad (9)$$

$$\frac{dP_s^\pm(z)}{dz} = \Gamma_s N_2 \left[(\sigma_{as}f_{es} + \sigma_{es}f_{us}) - \sigma_{as}f_{es}N \right] P_s^\pm(z) - \alpha_s P_s^\pm(z) \quad (10)$$

with the boundary condition

$$P_s^+(0) = R_1 P_s^-(0), \quad (11)$$

$$P_s^-(L) = R_2 P_s^+(L) \quad (12)$$

where the superscript of P_s^\pm and P_p represent the propagation direction for the power along the fiber, the positive superscript represents forward direction and the negative superscript represents backward direction of laser beam and L is the fiber length.

α_p and α_s are scattering loss coefficients of pump light and laser light respectively. R_1 and R_2 are the power reflectivity of Fabry Perot reflectors at laser wavelength at $z = 0$ and $z = L$, respectively. From above equations, the numerical results of power distribution along the fiber laser can be calculated.

The temperature distribution of fiber core T_1 and fiber cladding T_2 respectively, as a function of fiber radius and fiber length and can be given as [24]:

$$T_1(r, z) = T_c + \frac{Q(z)}{4\kappa} (a^2 - r^2) + \frac{Q(z)}{2\kappa} a^2 \left(\ln\left(\frac{d}{a}\right) + \frac{\kappa}{dh_c} \right) \quad (0 \leq r \leq a) \quad (13)$$

$$T_2(r, z) = T_c + \frac{Q(z)a^2}{2\kappa} \left(\ln\left(\frac{d}{a}\right) + \ln\left(\frac{r}{a}\right) \right) + \frac{Q(z)a^2}{2dh_c} \quad (a \leq r \leq d) \quad (14)$$

where $Q(z)$ is the heat power density, κ represents thermal conductivity, T_c is environment temperature and h_c is the heat transmission coefficient of the fiber surface.

3- RESULTS AND DISCUSSION

Numerical simulations are carried out by solving the rate equations to study the effects of temperature variation on the performance of high power YDFs. The parameters used in the simulations are included in Table 1. The variations of output power with pump power for 915 nm and 970 nm signals at different temperatures 253k, 293k and 333k are shown in Figure 2 and 3 respectively. It is clear from the results that increasing the pump power will increase the output power. At the same time the output power decreases with increasing temperature from 253k to 333k which agrees with previous results and can be explained by the fact that as the population of the sublevel "a" decreases with the increase in temperature, while the population of sublevel "c" increases, that is the absorption of pump declines and the absorption of laser rises [13,14].

The variations of output power with fiber length for 915 nm and 970 nm signals at different temperatures (243k & 363k) with the pump power of 1500 W are shown in Figure 4 and 5 respectively. It is clear from the results that the optimal fiber length is about 12 m. According to Figs. 3 and 4, when the fiber length is longer, the difference of output power at difference temperature becomes smaller and smaller as shown in Figures 4 and 5 respectively. This indicates that the effect of temperature is the smallest when the pump power is absorbed entirely.

Table 1 Parameters used in the simulation.

Parameters	Value
Signal wavelength (λ_s)	1100nm
Pump wavelength (λ_p)	915,970nm
Yb ion density (N)	$80 \times 10^{24} \text{ m}^{-3}$
Numerical aperture (NA)	0.2nm
Excited-state lifetime (τ)	0.8ms
Core radius	2.5 μ m
Environment temperature (T_c)	298k
Heat transmission coefficient (h_c)	17W/(m ² K)
Thermal conductivity (κ)	1.38 W/(mK)
Scattering loss coefficient of laser light (α_s)	5×10^{-3}
Scattering loss coefficient of pump light (α_p)	3×10^{-3}
Absorption cross section at pump wavelength (σ_{ap})	$2.5 \times 10^{-24} \text{ m}^2$
Absorption cross section at laser wavelength (σ_{as})	$1.5 \times 10^{-26} \text{ m}^2$
Emission cross section at pump wavelength (σ_{ep})	$2.5 \times 10^{-24} \text{ m}^2$
Emission cross section at laser wavelength (σ_{es})	$3.2 \times 10^{-25} \text{ m}^2$

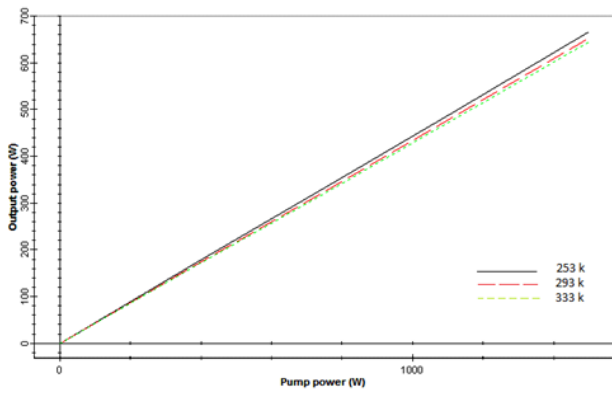


Figure 2 Output power as a function of pump power (915nm) for different temperature when $L = 3$ m.

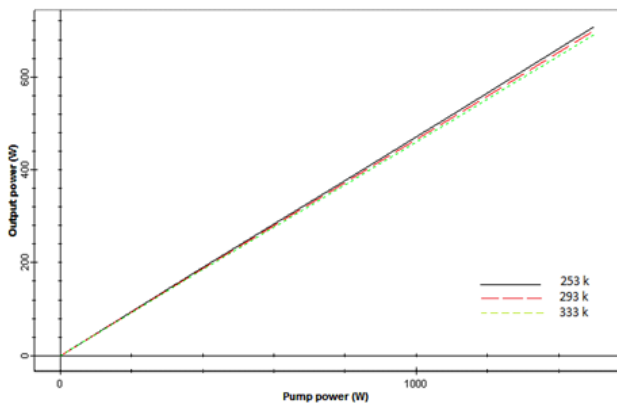


Figure 3 Output power as a function of pump power (970nm) for different temperature when $L = 3$ m.

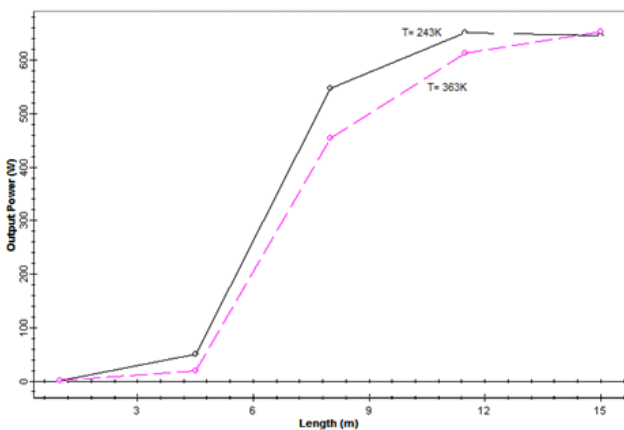


Figure 4 The output power as a function of fiber length for different temperature when Pump power = 1500 W for 915nm signal

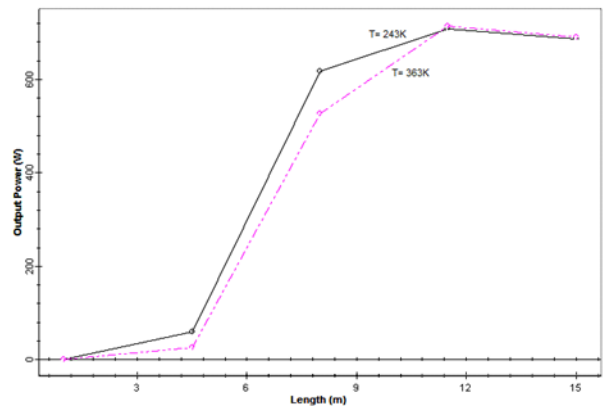


Figure 5 The output power as a function of fiber length for different temperature when Pump power = 1500 W for 970nm signal

The variation of the output power with the fiber length for different pump power for 915nm and 970nm signals are shown in Figures 6 and 7 respectively. It is clear from the results that the output power increases with increasing pump power. The optimal length for different pump power is around 12m.

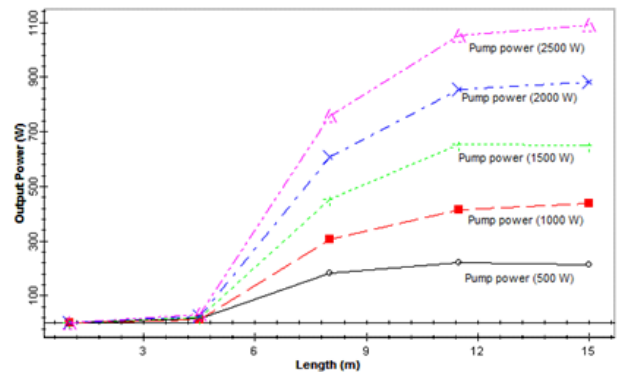


Figure 6 The output power as a function of fiber length at room temperature (273k) for 915nm signal.

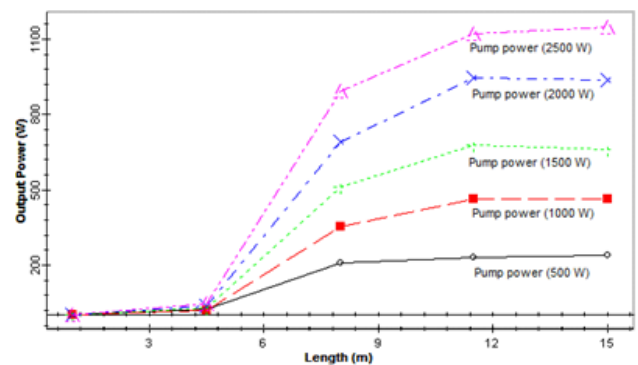


Figure 7 The output power as a function of fiber length at room temperature (273k) for 970nm signal.

4- CONCLUSION

This paper has described in detail a temperature-dependent model for (YDFL) based on Fabry-Perot design. The output performance mainly the output power of YDFL variation with temperature is investigated. It is clear from the results that the output power decreases with the increase of temperature. Moreover, the variation of output power with temperature increases with the increase of the pump power. The theoretical results obtained here is in agreement with the published experimental result. These results show that the temperature effect must be considered especially when the laser is operated at higher pump power.

REFERENCES:

- [1] H. W. Etzel, H. W. Candy, and R. J. Ginther, "Stimulated emission of infrared radiation from ytterbium-activated silicate glass," *Appl. Opt.*, vol. 1, pp. 534, 1962.
- [2] R. Paschotta, J. Nilsson, A. C. Tropper, and D. C. Hanna, Ytterbium-Doped Fiber Amplifiers, *IEEE journal of quantum electronics*, vol. 33, no. 7, pp. 1049-1056, JULY 1997.
- [3] J. Chen, Z. Sui, F. Chen and J. Wang, Output characteristics of Yb³⁺-doped fiber laser at different temperatures, *Chin. Opt. Lett.*, vol. 4, no. 3, pp. 173-174, (2006).
- [4] M. J. F. Digonnet, Rare-Earth-Doped Fiber Lasers and Amplifiers model for rare-earth-doped fiber amplifiers and lasers, CRC Press; 2nd edition (2001).
- [5] J. Yi, Y. Fan, S. Huang, Study of Short-Wavelength Yb: Fiber Laser, *Photonics Journal*, vol. 4, no. 6, pp. 2278 - 2284, (2012).
- [6] B. Zhang, R. Zhang, Y. Xue, Y. Ding, and W. Gong, Temperature Dependence of Ytterbium-Doped Tandem-Pumped Fiber Amplifiers, *Photonics Technology Letters*, vol. 28, no. 2, pp. 159-162, (2016).
- [7] H. M. Pask, R.J. Carman, D. C. Hanna, A. C. Tropper, C. J. Mackechinc, P. R. Barber, and J. M. Dawes, *IEEE Sel. Top. Quantum Electron.* 1, 2 (1995).
- [8] L. Yan, W. Chunyu, L. Yutian, A four-passed ytterbium-doped fiber amplifier, *Optics & Laser Technology*, pp. 1111-1114 39 (2007).
- [9] J. Y. Allain, J. F. Bayon, M. Monerie, P. Bernage, and P. Niay, Ytterbium-doped silica fiber laser with intracore Bragg gratings operating at 1.02 μm , *Electron. Lett.*, vol. 29, no. 3, pp. 309-310, (1993).
- [10] Y. Jeong, J. K. Sahu, D.N. Payne, J. Nilsson, Ytterbium-doped large-core fiber laser with 1 kW of continuous-wave output power *electronics letter* vol. 40, no. 8, pp. 470-472, (2004).
- [11] Y. Wang, Thermal effects in kilowatt fiber lasers, *IEEE Photonics Tech. Lett.* 16, pp. 63-65, (2004).
- [12] J. X. Chen, Z. Sui, F.S. Chen, *Opto-Electron. Eng.* 32, pp. 77-79, (2005).
- [13] Q. J. Jiang, P. Yan, J.G. Zhang, M.L. Gong, Analysis on thermal characteristic of Ytterbium-doped fiber laser, *Chin. J. Laser* 35, pp. 827-829, (2008).
- [14] N. A. Brilliant, and K. Lagonik, Thermal effects in a dual-clad ytterbium fiber laser, *Opt. Lett.* 26, pp. 1669-1671, (2001).
- [15] D. A. Gruk, A. S. Kurkov, V. M. Paramonov, E. M. Dianov, Effect of heating on the optical properties of Yb³⁺-doped fibers and fiber lasers, *Quant. Elect.* 34, pp. 579-582, (2004).
- [16] L. J. Henry, T. M. Shay, D. W. Hult and K. B. Rowland Jr, Thermal effects in narrow linewidth single and two tone fiber lasers, Vol. 19, no. 7, *Optics express* 6165, (2011)
- [17] B. K. Zhou, Principle of Laser, sixth ed., National Defense Industry Press, China, 2008.
- [18] X. Peng, L. Dong, Temperature dependence of ytterbium-doped fiber amplifiers, *J. Opt. Soc. Am. B* 25, pp. 126-130, (2008).
- [19] A. H. M. Husein, A. H. El-Astal, F.I. El-Nahal, The gain and noise figure of Yb Er-codoped fiber amplifiers based on the temperature-dependent model, *Opt.Mater.* 33, pp. 543-548, (2011).
- [20] A. H. M. Husein, F. I. El-Nahal, Model of temperature dependence shape of ytterbium -doped fiber amplifier operating at 915 nm pumping configuration, (*IJACSA*) International Journal of Advanced Computer Science and Applications, vol. 2, no. 10, pp. 10-13, (2011).
- [21] T.Y. Fan, Optimizing the efficiency and stored energy in quasi three-level lasers, *IEEE J. Quant. Elect.* 28, pp. 2692-2697, (1992).
- [22] B. Majaron, H. Lukac, M. Copic, Population dynamics in Yb:Er: phosphate glass under neodymium laser pumping, *IEEE J. Quant. Elect.* 31, pp. 301-308, (1995).
- [23] J. T. Fournier and R. H. Bartram, "Inhomogeneous broadening of the optical spectra of Yb³⁺ in phosphate glass," *J. Phys. Chem. Solids*, vol. 31, pp. 2615-2624, (1970).
- [24] D. C. Brown, H. J. Hoffman, Thermal, stress, and thermo-optic effects in high average power double-clad silica fiber lasers, *IEEE J. Quant. Electron.* 37, pp. 207-217, (2001).